



Multi-frequency satellite radar imaging of cultural heritage: the case studies of the Yumen Frontier Pass and Niya ruins in the Western Regions of the Silk Road Corridor

Fulong Chen, Nicola Masini, Jie Liu, Jiangbin You & Rosa Lasaponara

To cite this article: Fulong Chen, Nicola Masini, Jie Liu, Jiangbin You & Rosa Lasaponara (2016): Multi-frequency satellite radar imaging of cultural heritage: the case studies of the Yumen Frontier Pass and Niya ruins in the Western Regions of the Silk Road Corridor, International Journal of Digital Earth, DOI: [10.1080/17538947.2016.1181213](https://doi.org/10.1080/17538947.2016.1181213)

To link to this article: <http://dx.doi.org/10.1080/17538947.2016.1181213>



Published online: 19 May 2016.



Submit your article to this journal [↗](#)



View related articles [↗](#)



View Crossmark data [↗](#)

Multi-frequency satellite radar imaging of cultural heritage: the case studies of the Yumen Frontier Pass and Niya ruins in the Western Regions of the Silk Road Corridor

Fulong Chen^{a,b}, Nicola Masini^c, Jie Liu^{a,b}, Jiangbin You^a and Rosa Lasaponara^{a,d}

^aKey Laboratory of Digital Earth Science, Institute of Remote Sensing and Digital Earth, Chinese Academy of Sciences, Haidian District, Beijing, People's Republic of China; ^bInternational Centre on Space Technologies for Natural and Cultural Heritage under the Auspices of UNESCO, Haidian District, Beijing, People's Republic of China; ^cInstitute for Archaeological and Monumental Heritage, National Research Council, Tito Scalo, PZ, Italy; ^dInstitute of Methodologies for Environmental Analysis, National Research Council, Tito Scalo, PZ, Italy

ABSTRACT

Synthetic Aperture Radar (SAR) remote sensing is increasingly favoured in archaeological applications. However, the effectiveness of this technology for archaeological prospection has so far not been fully assessed. In this study, an integrated single-date and multi-temporal SAR data-processing chain was proposed to sharpen archaeological signs and hence their detection and monitoring. In total, 14 scenes of X-band Cosmo-SkyMed, C-band Sentinel-1 and L-band PALSAR data covering the Western Regions of the Silk Road Corridor in China were employed for two important archaeological sites including the Yumen Frontier Pass with emerging archaeological traces and Niya ruins with subsurface remains. The results pointed out that single-date satellite radar data were useful for the identification of subsurface traces buried under desert in the landscape-scale, whereas for the identification of emerging monuments, Sentinel-1 was limited by its lower spatial resolution compared to TerraSAR and PALSAR data. Multi-date products, such as interferometric coherence, the averaged radar signatures and RGB multi-temporal composites, were effective to sharpen archaeological traces as well as for change detection in Yumen Frontier Pass. This study presents a pilot assessment of satellite SAR data for the analysis and monitoring of archaeological features in the predominantly arid-sandy environmental characteristic of investigated sites.

ARTICLE HISTORY

Received 1 March 2016
Accepted 18 April 2016

KEYWORDS

Archaeological prospection; Silk Road; SAR; Yumen Frontier Pass; Niya ruin; iron age

1. Introduction

Ancient human activities alter landscape and surrounding environments, leaving us archaeological traces that, although quite subtle, could be recognized from space even after centuries. Satellite multi-spectral sub-metric data provide challenging opportunities to improve the extraction of information, from the qualitative and quantitative point of view, also in the case of subtle signals with typical characterize buried and shallow archaeological remains. Actually, several well-known archaeological marks (including crop, soil and shadow signs) have been fruitfully used as proxy indicators of the presence of buried and surface archaeological remains through case studies mainly based on optical data (Crawford 1929; Masini and Lasaponara 2007; Parcak 2009; Keay, Parcak, and Strutt 2014). Actually, in the last 10 years the use of satellite optical imagery (Agapiou and Lysandrou 2015)

CONTACT Fulong Chen  chenfl@radi.ac.cn  Key Laboratory of Digital Earth Science, Institute of Remote Sensing and Digital Earth, Chinese Academy of Sciences, No. 9 Dengzhuang South Road, Haidian District, Beijing 100094, People's Republic of China

© 2016 Informa UK Limited, trading as Taylor & Francis Group

has shown great potentiality in archaeology for site detection and monitoring as well as for ‘landscape archaeology’ investigations so that a new research field is under development generally named ‘archaeology from space’ – that is the study of past settlements (buried or emerging) and landscape using satellite data.

Nowadays, the increasing availability of active and passive satellite sensors that provide very high-resolution data has opened new opportunities, unthinkable only a few years ago. The space technologies available today can provide extremely precise results for archaeological applications speeding up the work during the diverse phases of investigations ranging from survey, mapping, excavation, documentation, exploitation and monitoring. Moreover, satellite sensors offer data and information at diverse scales of interest, moving from small artefacts to architectural structures and landscape reconstruction. It is also possible to integrate ancient environment reconstruction, obtainable from space, with the mapping of past (even buried) and present (emerging) settlements and landscapes.

Synthetic Aperture Radar (SAR), in comparison with optical approaches, is an innovative microwave remote-sensing technology characterized by penetration, polarization and interferometry. More recently, different methodologies based on both single-date and multi-temporal data analysis, exploiting the backscattering and the penetration of spaceborne radar data have been used for studies on several archaeological sites and landscapes (Cigna et al. 2013; Lasaponara and Masini 2013, 2015; Stewart, Lasaponara, and Schiavon 2013, 2014; Chen, Lasaponara, and Masini 2015; Chen, Masini, et al. 2015). The mission of SIR-C/X-SAR allowed a systematic measurement and estimation of radar backscattering signature of the Earth’s surface from space at different frequencies and polarizations owing to the technology and methodology development (Schaber, McCauley, and Breed 1997; Narayanan and Hirsave 2001; Ranson et al. 2001). Up to now, the performance and capability of current spaceborne SAR in archaeological prospection have not been fully assessed although several pilot studies have been conducted using the in-orbit X-band TerraSAR data (Linck et al. 2013; Erasmi et al. 2014; Chen, Masini, et al. 2015), and laboratory studies and modelling (Morrison 2013). SAR techniques enable us to overcome some limitations of optical imaging providing (i) all weather acquisitions, (ii) at any time of day or night and (iii) capable to ‘penetrate’ (to some extent) vegetation and/or soil depending on the antenna wavelength, surface characteristics (ice, desert sand, close canopy, etc.) and conditions (moisture content). However, a correct identification and interpretation of archaeological features (marks) on the basis of radar images is not a straightforward task and requires knowledge about ground surface conditions as well as about the interaction mechanisms between radar waves and surface sensed.

To provide a contribution to this novel research line, in this study, an integrated single-date and multi-temporal SAR data-processing chain was proposed to investigate archaeological signs in some significant test sites located in China along the so-called Silk Road to demonstrate the performance and potential of satellite SAR data for future archaeology along this routine as well as in South America, Africa and Central/Western Asia with analogous arid-sandy environment.

2. SAR in archaeology

In the past, archaeological research based on satellite SAR data was constrained by low-resolution as well as complexity of data processing and interpretation. Today, abundant high resolution, multi-mode satellite SAR, that is, TerraSAR/TanDEM-X, Cosmo-SkyMed, Radarsat-2 and ALOS PAL-SAR-2, as well as SAR data that are cost-free (Sentinel-1 from European Space Agency) are available due to the technology development for acquiring multi-mode data. SAR data for archaeology definitely could step into a golden era, but applications still face challenges due to the lack of systematic methodologies for acquiring and interpreting data. For example, compared with optical approaches, performance of SAR data for archaeological applications is not fully understood and needs exploitation for further advancing the use of the technology.

Firstly, archaeological sites with regular, observable topological traces on the landscape – for example, crop, shadow, soil and damp marks (Lasaponara and Masini 2013; Chen, Masini, et al.

2015) – create anomalies on the images, implying the potential of remote sensing for archaeology, particularly when high-resolution SAR data – for example, TerraSAR/TanDEM-X, Cosmo-SkyMed, Radarsat-2 and ALOS PALSAR-2 – are used. Archaeological features, such as unknown palaeochannels buried under the desert, can be detected by SAR data, taking advantage of SAR's penetration capability (McCauley et al. 1982). In general, penetration is stronger as radar wavelength and subsurface porosity increase. In view of the complicated scenario, the quantitative penetration depth of SAR data however needs to be further estimated through a sufficient number of case studies.

Scaling effect related to the resolution of SAR images is another scientific issue. The optimization of image scaling contributes for cost-savings and for improving detection performance in archaeological applications; for example, moderate-resolution SAR data are suitable for large-scale heritage sites and their surrounding palaeoenvironment, and high-resolution data are critical for specific local-scale ruins.

The geometry of SAR imaging (i.e. incidence angle together with satellite flight path) has a close relationship to surface backscattering. Compared with incidence angle, the impact of satellite flight path (ascending and descending acquisitions) is more significant in archaeological applications because of the interactions between the sensitivity of radar echoes and linear features on the earth's surface. Strong linear backscattering anomalies on SAR images can be observed when the flight path is approximately parallel with linear archaeological features.

Images from multi-mode (e.g. multi-frequency, multi-temporal and multi-polarization) SAR platforms provide different sensed parameters, which is beneficial for the detection of archaeological remains. However, the heterogeneity of data brings in the complexity of image processing and interpretation. For instance, the scattering mechanism that determines the relationship between radar waves and surface/subsurface echoes needs to be investigated for the SAR data optimization. Moreover, the normalization of multi-mode SAR data is also essential for the performance comparison and assessment.

Apart from the local-scale archaeological signs (crop, soil and shadow), ancient ruins alter regional landscape that could be observed by remote-sensing images and derived added-value products, resulting in the rise of a new sub-discipline of Landscape Archaeology (Ashmore and Blackmore 2008; Keay, Parcak, and Strutt 2014). Landscape analysis is becoming an irreplaceable component in SAR remote sensing for archaeology. Considering the relationship between the occurrence of ancient ruins and topography, such as those located in high-level wetland platforms (Garrison et al. 2011), SAR-interferometry-derived Digital Elevation Model (DEM) can be used for identifying potential sites.

3. Study site and data

3.1. Study area

Silk Road is a series of ancient trade and cultural transmission routes connecting China to Europe in the Iron Age. It is witness to a civilization friendship and harmony between the East and West dating back to 2000 years, that has left us with various relics (e.g. lost cities) still unknown to be uncovered and investigated (Chen, Lasaponara, et al. 2015). Silk Roads: the Routes Network of Chang'an-Tianshan Corridor, running across China, Kazakhstan and Kyrgyzstan, has been inscribed in the UNESCO World Heritage List in 2014. Following the orders of the Han Emperor Wudi (156 BC–87 BC), envoy Zhang Qian undertook two different journeys to open the Southern and Central Routes of the Silk Road (first journey: 139 BC–126 BC; second journey: 119 BC–115 BC). Since 60 BC, the Western Han established the Protectorate of the Western Regions in Wulei (near the present Luntai County, Xinjiang) to supervise regimes in the vast area, which protected the merchants and travellers along the Silk Road, making trade more prosperous and busy. As the artery for the implementation of the Silk Road Economic Belt (SREB) initiative in China, archaeological heritage along the Silk Road (which are increasingly impacted by accelerated, on-going urbanization) has

become a public concern in aspects of detection, monitoring as well as conservation through multi-disciplinary investigation (Bonavia 2004; Hill and Fan 2009) since the beginning of this new millennium (Yilmaz, Yakar, and Yildiz 2008; Liu et al. 2011, 2012; Rondelli, Stride, and Garcia-Granero 2013; Wang and Zhao 2013; Luo et al. 2014). However, archaeological prospection for this corridor confronts the challenges of wide spatial coverage (e.g. extending across approximately 7000 km) and diversified ecological environments – for example, from the semi-humid continental monsoon climate in the east to the Mediterranean climate in the west. In the framework of the Chinese-Italian bilateral project and the Hundred Talents Program of the Chinese Academy of Sciences, some pioneering investigations on the Western Regions along the Silk Road in Western-Han Dynasty (202 BC–AD 8) have been undertaken by using multi-source satellite SAR data. The Tarim Basin between the Tianshan Mountains to the north and Kunlun Mountains to the south as well as the eastern entrance of Yumen Frontier Pass was the focus in this study. This area is surrounded by mountains, deserts, Gobi and oases, covering 26 of the 36 regimes in the Western Regions in Western-Han Dynasty (see Figure 1: known capital cities of the regimes are marked by red circles and others are marked by blue circles). The climate here is extremely dry with its annual precipitation less than 50 mm compared to annual transpiration of larger than 1500 mm generally. Two representative study sites, including Yumen Frontier Pass with emerging remains on the Gobi and Yadan landscape and Niya ruins with buried remains covered by desert sand, were selected for detailed investigations.

3.2. Satellite data

Three scenes of TerraSAR-X, one scene of Sentinel-1 and six scenes of ALOS PALSAR data in Yumen Frontier Pass; two scenes of ALOS PALSAR, one scene of Sentinel-1 and one scene of Cosmo-SkyMed data in Niya ruins of Jingjue regime were collected for archaeological investigations. Acquisition parameters of multi-source SAR data are listed in Table 1. Note that the polarization

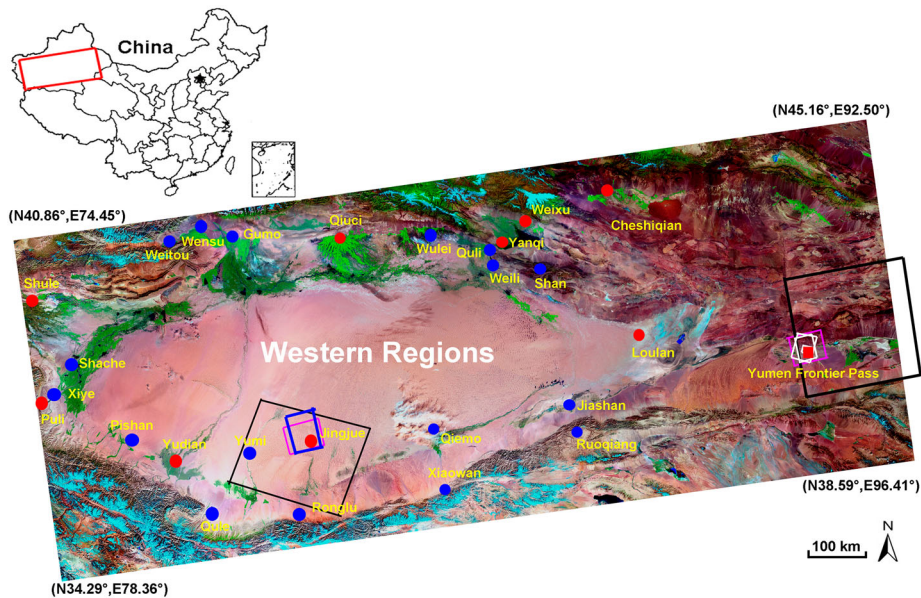


Figure 1 Study site of the Western Regions (marked by the red rectangle on the administrative map of China) in Western-Han Dynasty overlapped on mosaic Landsat ETM imagery. Twenty-six capital cities of the 36 regimes were marked by red circles (known) and other cities are indicated in blue. The Yumen Frontier Pass is indicated by the red square. Spatial coverage of PALSAR, Sentinel-1, Cosmo-SkyMed and TerraSAR data on two selected sites (Yumen Frontier Pass and Niya ruins) is shown by pink, black, blue and white rectangles, respectively.

Table 1. Acquisition parameters of SAR data used in this study.

Site	Satellite	Acquisition	Polarization	Inc. angle	Spatial extent (km ²)
Yumen Frontier Pass	TerraSAR-X	Stripmap: 23 September 2012, descending; 28 April 2013, ascending	VV	40°	30 × 50
		Spotlight: 6 October 2014, descending	HH	22°	10 × 5
	Sentinel-1 PALSAR	17 October 2014	VV	39°	250 × 200
		FBS: 30 March 2008, 31 December 2008, 21 February 2011	HH	34°	60 × 70
		FBD: 28 June 2007, 30 September 2008, 6 October 2010	HH/HV		60 × 70
Niya ruins	Cosmo-SkyMed	18 March 2015	HH	29°	40 × 40
	Sentinel-1 PALSAR	22 March 2015	VV	39°	250 × 200
		4 July 2007, 19 August 2007	HH/HV	34°	60 × 70

difference of SAR datasets could be neglected considering the co-polarized images applied in this study. L-band (23.6 cm wavelength) ALOS PALSAR data, ascending mode with an incidence angle of 34° were acquired on 4 July 2007 and 19 August 2007 for Niya ruins and for the period from 28 June 2007 to 21 February 2011 for Yumen Frontier Pass, respectively. PALSAR has two fine acquisition modes – including Fine Beam Single polarization (FBS, range bandwidth of 28 MHz) in HH polarization and Fine Beam Dual polarization (FBD, 14 MHz) in HH/HV dual polarization, respectively. The ground resolution is 8 m for FBS and 16 m for FBD with an incidence angle of 34° (note that only the common HH channel from FBS and FBD was used in this study). C-band (5.6 cm wavelength) Interferometric Wide Swath (IW) Sentinel-1 data, VV polarization with an incidence angle of 39°, descending mode were acquired on 22 March 2015, for Niya ruins, and ascending mode acquired on 17 October 2014 for Yumen Frontier Pass. The ground resolution of IW Sentinel-1 data is approximately 5 × 20 m. X-band (3.1 cm wavelength) TerraSAR data, including Stripmap (3 m ground resolution) and Spotlight (1 m ground resolution), were acquired on 23 September 2012 (descending), 28 April 2013 (ascending) and 6 October 2014 (descending), respectively, for Yumen Frontier Pass, and Cosmo-SkyMed Stripmap (ascending, 3 m ground resolution) acquired on 18 March 2015 for Niya ruins. Furthermore, thematic archaeological layer of Niya ruins up to 2000 (provided by Archaeological Institute of Xinjiang Uygur Autonomous Region) was acquired for the performance assessment of SAR data. DEM generated from TerraSAR/TanDEM-X bistatic CoSSC data was used for the topographic analysis of landscape in Niya ruins. The software tool of ‘Interferometric DEM generation with TerraSAR-X + TanDEM-X bistatic data’ in SARscape 5.1 was applied for the CoSSC data processing. Generally, the satellite constellation of TerraSAR/TanDEM-X allows the generation of DEM with an unprecedented accuracy conforming to the High-Resolution Terrain Information-3 (HRTI-3) specification – that is, absolute horizontal accuracy <10 m, relative vertical accuracy <3 m. In this study, a high-resolution DEM can be guaranteed (particularly in the relative vertical accuracy), although the corresponding accuracy was inferior to the HRTI-3 specification considering one image pair was processed only.

4. Data processing and methodology

4.1. Rationale

In this study, X-, C- and L-band satellite SAR datasets were firstly applied for the analysis and monitoring of archaeological features to assess the capability of multi-mode SAR data in archaeological applications.

The extraction of archaeological features from SAR data is a challenging task. One of the main problems for the processing and interpretation of SAR data lies in the fact that backscattering includes interlinked information on soil moisture, surface roughness, target orientation, shape

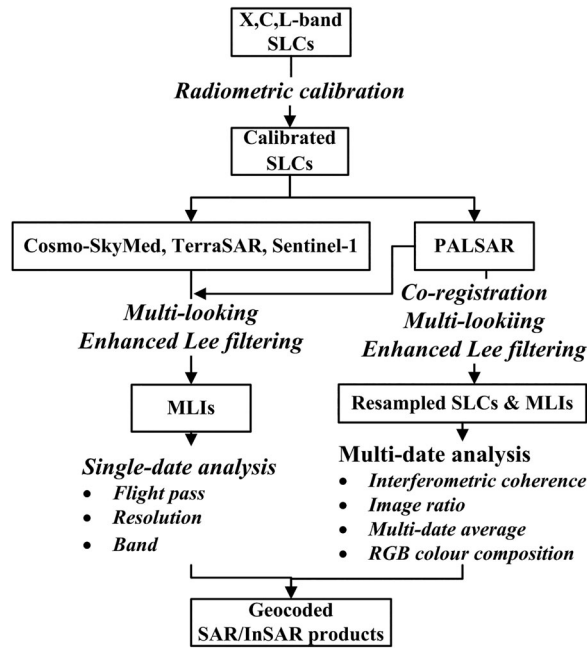


Figure 2. Multi-source satellite SAR data-processing and performance-assessment approaches used in this study for archaeological prospection in the Western Regions along the Silk Road.

and material. Parameterization and/or isolation of these diverse contributions from the overall scattering data have attracted considerable research topic over decades (Shi et al. 2012) and continue to be of great interest. This is particularly important when, for example, surface soil moisture is a key parameter that can strongly influence the visibility of archaeological marks as well as the SAR penetration capability. Moreover, additional issues are the low Signal-to-Noise Ratio (SNR), especially considering the complexity of the archaeological targets and the fact that other features of modern landscapes may mask them. In this study, for the SAR data assessment in archaeological prospection of the Silk Road in terms of spatial resolution, imaging geometry, radar frequency and time of acquisitions, a SAR data-processing framework was designed for L-band PALSAR, C-band Sentinel-1 and X-band TerraSAR and Cosmo-SkyMed with a view to sharpen archaeological signs (Figure 2) based on synergetic methodologies of single-date (Section 4.2) and multi-date (Section 4.3) processing following the fruitful results obtained by our team in a previous study focused on the use of Cosmo-SkyMed data (see Chen, Masini, et al. 2015). Note that multi-mode Single Look Complex data need to be radiometric calibrated in advance; multi-looking operators were applied for the amplitude data generation; and the enhanced Lee (Lopes, Touzi, and Nezry 1990) together with Goldstein filter (Goldstein and Werner 1998) was applied for the speckle suppression and interferogram filtering respectively in the following procedures of SAR data processing and analysis. To highlight the significance of multi-temporal assessment, herein four different SAR products were generated based on the co-registered PALSAR stack: (i) interferometric coherence, (ii) image ratios, (iii) averaged radar signatures and (iv) RGB colour composites. The specific approach to processing is dependent on the availability of data for the investigated sites.

4.2. Single-date X-, C- and L-band amplitude SAR analysis

Some of our recent investigations suggest that the use of X-band satellite SAR offers significant capability for the identification of archaeological signs (Chen, Masini, et al. 2015). Results obtained in

several study areas, characterized by diverse surface characteristics and land covers (desert, Mediterranean setting, etc.), suggested that shadow marks could be seen from single SAR data. Crop, soil and damp marks are generally more visible from optimal-selected single-date. This is due to the seasonal nature of the visibility of these archaeological features coupled with the low penetration capability of X-band; the match between soil properties and the acquisition parameters of the image itself is also important. Consequently, as in Chen, Masini, et al. (2015) speckle filtering is applied to enhance the SNR and Equivalent Number of Looks (ENL) of SAR data, and facilitates easier interpretation of archaeological features. There are several algorithms developed for SAR speckle filtering, for example, Lee (Lee 1980), enhanced Lee (Lopes, Touzi, and Nezry 1990), Front and Kuan filter (Shi and Fung 1994), which can suppress noise while at the same time preserving essential topological characteristics. On the basis of the previous results, single-date X-band TerraSAR, C-band Sentinel-1 and L-band PALSAR data were adapted for the performance assessment in this study through the comparison of (i) geometry of SAR imaging, (ii) spatial resolution of acquisition modes, (iii) different acquisition frequencies of X-, C- and L-bands.

4.3. PALSAR multi-temporal analysis

Multi-temporal PALSAR were firstly co-registered with accuracy up to subpixels. Then, four different typologies of products mentioned above were generated to analyse the radar backscattering properties and their evolution over the investigated sites. It is expected that the multi-temporal analysis will provide information on changed and unchanged areas and, in turn, on the presence of archaeological remains.

Along with the amplitude, the interferometric coherence between two or more SAR scenes can also provide additional, complimentary information about the scattering mechanisms on the surface. On the basis of an empirical approach, physical information may be recovered from the interferometric correlation coefficient, providing the presence/absence of variations between surface cover, moisture content, etc. In this study, the visibility of archaeological targets using ALOS PALSAR interferometric coherence γ were analysed; and Goldstein filter (Goldstein and Werner 1998) was applied for the noise mitigation:

$$\gamma = \frac{\sum_{n=1}^N s_{1n} \cdot s_{2n}^* \cdot \exp(-j\varphi_{flat,n})}{\sqrt{\sum_{n=1}^N |s_{1n}|^2 \cdot \sum_{n=1}^N |s_{2n}|^2}}, \quad (1)$$

where N is the number of pixels in the coherence window calculated, S_{1n} and S_{2n} are the complex value from master and slave image, respectively, $*$ indicates the conjugate operator and $\exp(-j\varphi_{flat,n})$ is the flat earth phase.

As demonstrated by several authors (Nico et al. 2000; Scheuchl, Ullmann, and Koudogbo 2009; Boldt and Schulz 2012), amplitude ratio information of SAR pairs acquired with the same parameters is helpful to enhance and map changes occurred over the imaged area. The rationale of such an amplitude-based approach is to assess the changes of each element on the ground based on its radar backscattering properties rather than on temporal interferometric coherence. An advantage of this approach is the possibility to cancel out the effects of topography on the radar backscattering. The formula that was employed, pixel by pixel, to compute the ratio R_{σ^0} between a pair of scenes k and j which were acquired at the times t_k and t_j , respectively is as follows:

$$R_{\sigma^0} = \frac{\sigma_i^0(t_k)}{\sigma_i^0(t_j)}. \quad (2)$$

The computation of the temporal average image based on co-registered multi-date scenes allows the reduction of speckle noise and filtering out temporally uncorrelated signals, but preserves information on the physical properties of the imaged scene and the input spatial resolution. For each

image pixel i , the following formula was used to retrieve its average backscattering coefficient $\bar{\sigma}_i^0$:

$$\bar{\sigma}_i^0 = \frac{1}{n} \sum_{t=t_0}^{t=t_n} \sigma_i^0(t), \quad (3)$$

where t_0 and t_n are the times of acquisition of the first and last PALSAR scene, n is the total number of scenes composing the stack and $\sigma_i^0(t)$ is the radar backscattering coefficient of the pixel at the time t . For multi-temporal acquisitions covering the same observed scenario, multi-dates average is also useful to mitigate speckle noise through the enhancement of ENL. Generally, the ENL of imagery produced by averaging n SAR images could be increased by a factor of \sqrt{n} . Therefore, it is expected that use of multi-date average can enable us to easily identify and better characterize the archaeological features linked to buried and/or shallow remains.

Generation of RGB (Red–Green–Blue) colour composites of three radar images acquired at different times can ease the identification of any changes in the radar scattering properties over time. After the RGB colour composite generation, pixels characterized by constant values of the radar backscattering over time are shown with a grey scale, with brighter areas indicating more reflective targets, and darker pixels indicating areas of lower backscattering properties. On the other hand, any temporal change in the backscattering coefficient appears as coloured in the respective tint of the scenes which recorded the change.

5. Results

Two representative sites in the Western Regions (Western-Han Dynasty) along the Silk Road, including Yumen Frontier Pass with emerging remains and Niya ruins of Jingjue regime with sub-surface relics, were used to assess the capability of existing spaceborne SAR data for archaeological prospection.

5.1. Yumen Frontier Pass with emerging remains

Yumen Frontier Pass, together with Yang Frontier Pass, is one of the two important passes on the western frontier of the Han Dynasty (206 BC–AD 220) lands. Today, Yang Frontier Pass (located at around 75 km on the southwest side of Dunhuang) is only ruins, whereas the Yumen Frontier Pass still exhibits its impressive mud walls with around 10-m-high and its four gateways (Figure 3d). Gobi and Yadan topography is well developed here where the surface is formed by 2–3-m thick gravels without any plants and/or is mainly composed of salt encrustation with wind erosion. Yumen Frontier Pass was successfully added to the World Heritage List On June 22 2014. It is located at around 80 km northwest of Dunhuang in the Gansu Province, at the western end of Hexi Corridor. In ancient times, it was the crucial gateway from central China to the western regions; all caravans travelling through Dunhuang were required to pass through the Yumen Frontier Pass or the Yang Frontier Pass. The site was lost, re-discovered in 1907 by Sir Aurel Stein and investigated starting from 1944 by Chinese archaeologists.

As illustrated in Figure 1 and described in Table 1; three scenes of X-band TerraSAR, one scene of C-band Sentinel-1 and six scenes of L-band ALOS PALSAR data were applied for the investigation. The acquisition time difference of multi-source SAR datasets could be ignored, considering the arid-dry climate throughout of the year. All SAR data were filtered by the enhanced Lee operator (3×3 window size) for the speckle noise suppression. First, the acquisitions of ascending (28 April 2013) and descending (23 September 2012) Stripmap TerraSAR images with approximately uniform incidence angle (40°) were employed to test the performance of imaging geometry. Although similar backscattering and topology of the pass were observed, the linear Han Great Wall was reflected more clearly on the ascending acquisition than on the descending one; this is probably due to the parallel flight path of the ascending acquisition compared with the direction of the Han Great

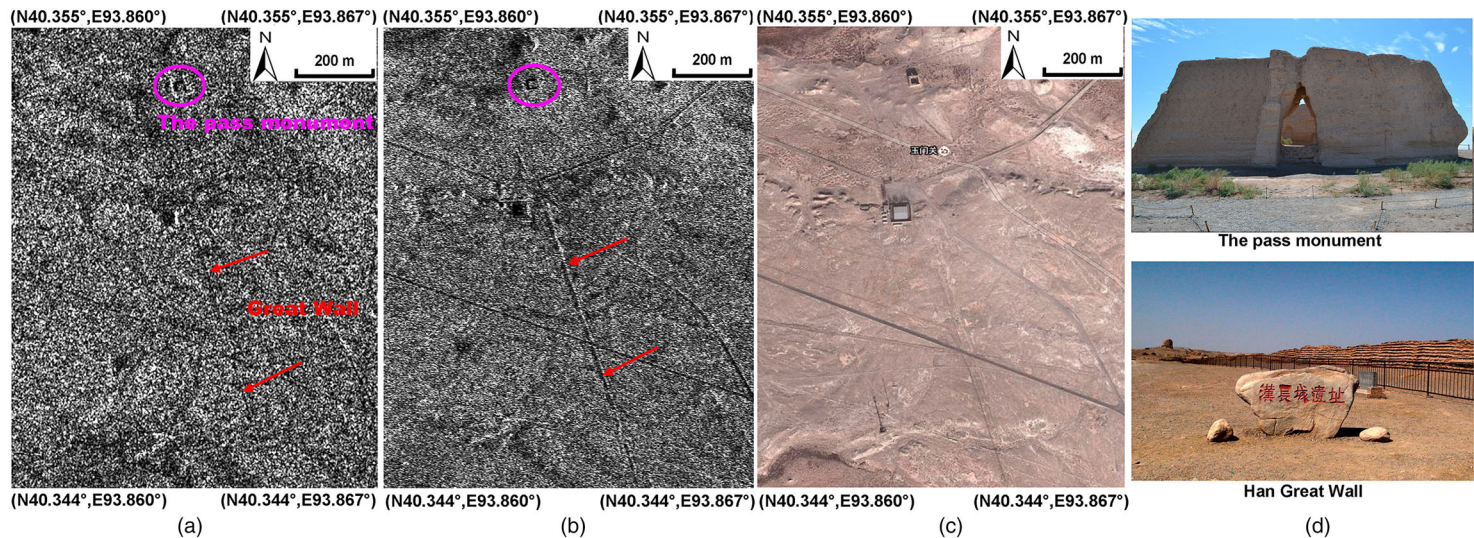


Figure 3. Comparison of TerraSAR-X data between Stripmap (a), descending with 3 m resolution and Spotlight (b), descending with 1 m resolution. It indicates that higher resolution remote-sensing data contributes more to archaeological interpretation than lower. (c) Optical imagery from Google Earth; (d) photos of the pass and Han Great Wall from field investigations.

Wall (see details in Chen, Lasaponara, and Masini 2015). Second, the capability of spatial resolution was estimated by comparing the Spotlight (1 m) with Stripmap (3 m) SAR data. Leaving out the impact of incidence angle (22° vs. 40°), it is clear that higher spatial resolution is beneficial for archaeological interpretation, proved by the distinct topological visualization of the pass and Great Wall in the Spotlight SAR image. Moreover, the advantage of SAR data for detection emerging remains was identified, particular for the linear rammed earth Great Wall located in the Gobi and Yadan landscape. It introduces the spectrum confusion in optical approaches and nevertheless results in the sharpened dihedral backscattering in SAR images (Figure 3).

Figure 4 shows the performance of X-band Stripmap TerraSAR, C-band Sentinel-1 and L-band PALSAR data for detection of the relics of Han Great Wall and Yumen Frontier Pass. First, it is evident that the spatial resolution could be the primary detecting factor because the shape of archaeological feature declines as the spatial resolution decreases. That is, the evident and continuous trace was observed in TerraSAR-X image (a); clear but discontinuous trace in PALSAR (b) while totally indiscernible in Sentinel-1 (c). Second, the sensitivity of microwave to the surface roughness decreases as the wavelength increases. For instance, the man-made archaeological features mentioned above were distinguished compared to their surroundings in PALSAR images, interpreted by the smooth dark-tone scenario caused by the dominant mirror reflection using L-band SAR. Nonetheless, when the wavelength decreases, the Bragg backscattering becomes dominant and results in analogous image tones in the entire observed scenario (a and c), introducing the confusion for the relic's identification.

Four typologies of multi-temporal PALSAR products, including interferometric coherence (generated by 30 March 2008 and 31 December 2008), image ratio of 30 March 2008 and 31 December 2008, multi-data average of six acquisitions spanning from 30 March 2008 to 21 February 2011, and RGB composites of 30 March 2008, 31 December 2008 and 21 February 2011 were then analysed, as illustrated in Figure 5. High coherence can be observed in the rectangular man-made relic caused by the invariant backscattering, such as Yumen Frontier Pass as marked by the pink ellipse in (a). In contrast, only partial linear archaeological features can be identified, for example, Han Great Wall marked by the blue arrows in (a). It is interpreted by the backscattering variation between two interferometric acquisitions and the decline impact induced by the coherence data processing for the thin

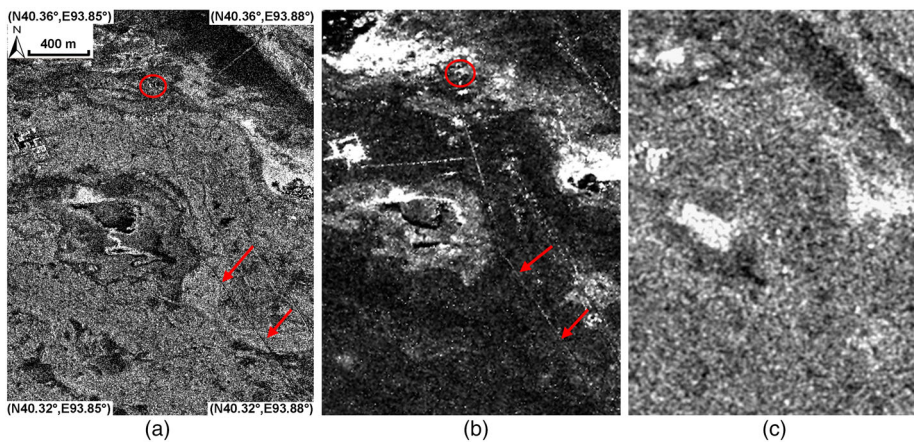


Figure 4. Performance assessment of X-, C- and L-band SAR data (filtered by a 3×3 pixel enhanced Lee operators) in detection of Han Great Wall and Yumen Frontier Pass. Note that the acquisition time difference of those data could be ignored, considering the invariant physical property of sensed relics impacted by the arid-dry climate. (a) X-band Stripmap TerraSAR with a spatial resolution of 3 m, (b) L-band PALSAR with a spatial resolution of 8 m and (c) C-band Sentinel-1 with a spatial resolution of 20 m. The Han Great Wall and relic of Yumen Frontier Pass were marked by red arrows and ellipses, respectively. Except for the spatial resolution, the optimal band of SAR data is determined by the discrimination of backscattering signature between archaeological features and their surroundings, such as the L-band PALSAR in this case.

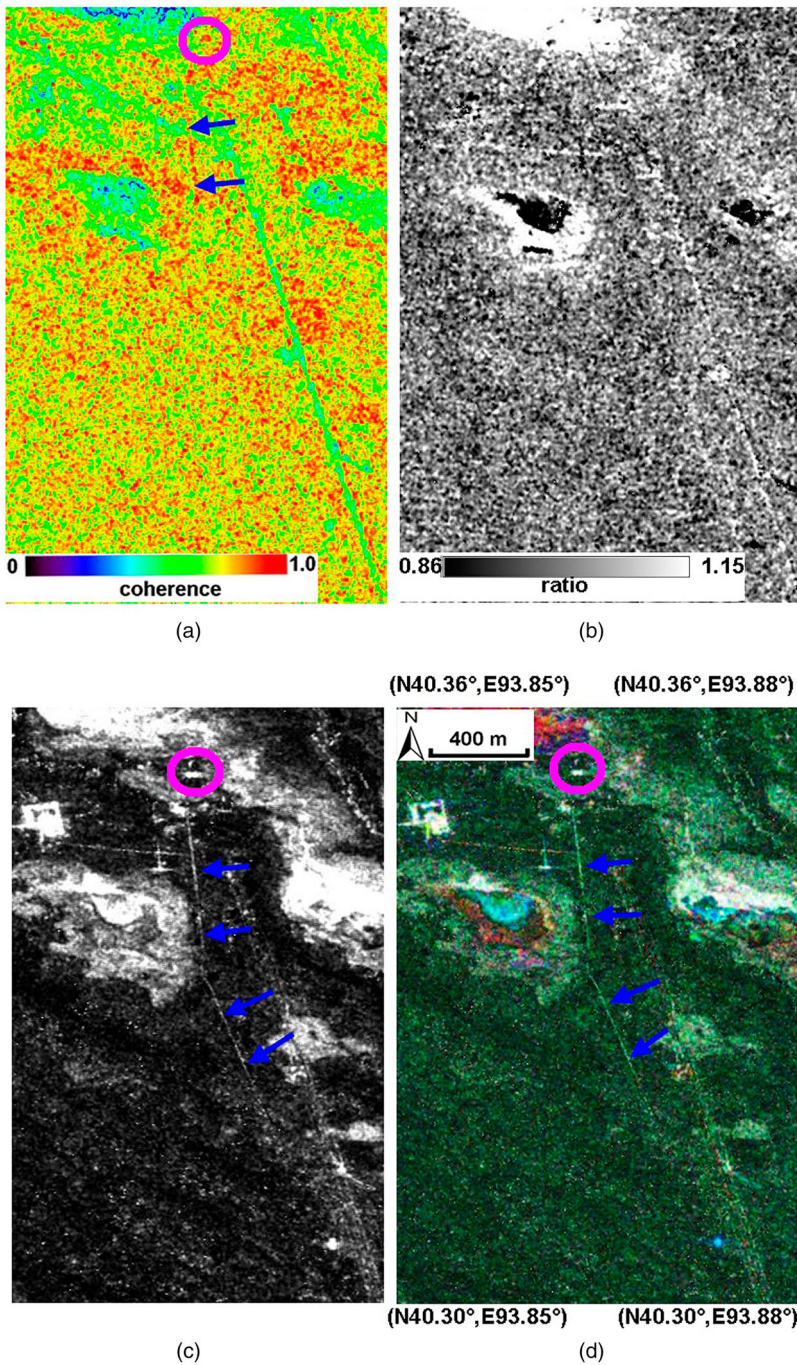


Figure 5. Multi-temporal processing of PALSAR to highlight the archaeological relics of Yumen Frontier Pass (marked by pink ellipses) and its surrounding Han Great Wall (marked by blue arrows). (a) Coherence image generated by 30 March 2008 and 31 December 2008, (b) image ratio of 30 March 2008 and 31 December 2008, (c) multi-date average of six acquisitions, (d) RGB composites of 30 March 2008, 31 December 2008 and 21 February 2011.

linear relic. In the image ratio (b), both the rectangular and linear archaeological relics could not be identified, interpreted the consistent moisture of the observed feature as well as the uniform imaging

geometry of SAR sensors. For the multi-date average (c) and RGB composites (d), both the rectangular and linear shape archaeological features were clearly observed. The speckle noise has been mitigated in (c) by temporal averaging, and archaeological relics showed as a grey scale in (d) due to the invariant backscattering in multi-temporal acquisitions.

5.2. Niya ruins with subsurface relics

Niya includes a group of towns located around what is now the dried bed of Niya River, in the southern region of the Taklamakan Desert, at the foot of the Kunlun Mountains. The archaeological site is approximately 115 km north of the modern Minfeng Town, Xinjiang, China. The surrounding landscape nowadays is predominated by migratory dunes in various shapes (e.g. crescent, barchans chain, strip and pyramid) and heights (e.g. ranging from 50 to 200 m). At the beginning, it was a military post under the Kingdom of Khotan, later it became an important oasis along the southern Silk Road and actually it was the site of Jingjue Kingdom in the Han and Jin Dynasties. Niya is thought to have achieved its high flourishing period between 200 BC and AD 500 – to be later abandoned, lost and buried in the desert sand, until re-discovered by Sir Aurel Stein at the beginning of the 20 centuries and later investigated by Chinese archaeologists. The ancient site (also called Eastern Pompeii) covers an area 25 km long from north to south and 5–7 km wide from east to west. The relics found within the site included houses, backyards, graveyards, stupa, Buddhist temple, fields, garden, pens for livestock, trenches, pottery kilns and smelting site. Unearthed were also carpentry, bronze, iron, pottery and stone wares, wool, coins and wooden slips. In order to protect the ruin, Niya was declared a state protected cultural relic site in 1996 and today access to the area is strongly restricted and only allowed by a special permit.

Totally, four acquisitions of SAR data, including one scene of X-band Cosmo-SkyMed image acquired on 22 March 2015, one scene of C-band Sentinel-1 image acquired on 22 March 2015 and two scenes of L-band FBD ALOS PALSAR images acquired on 4 July 2007 and 19 August 2007 (see [Figure 1](#) and [Table 1](#)) were used for the detection of unknown subsurface relics, taking advantage of the penetration capability of radar in dry-sandy landscape.

First, the performance of X-, C- and L-band SAR data was compared in discovery new archaeological remains. A suspected linear feature (highlighted by red arrows) was detected in the multi-frequency SAR images primarily owing to the penetration capability of SAR signature in this arid landscape, whereas no sign can be detected in WorldView-1 imagery of Google Earth, as illustrated in [Figure 6](#). It is clear that the C-band Sentinel-1 image with moderate spatial resolution (e.g. 20 m) (b) obtained the entire sketch of the linear feature because its physical backscattering (dominant dihedral backscattering) and the surroundings (Bragg backscattering) obtained an optimum discrimination, considering the roughness and moisture of the observed surface/subsurface. For the X-band Cosmo-SkyMed and L-band PALSAR SAR data, the performance in discrimination was suppressed (e.g. only section of the linear feature was detected) as a result of the interaction of the applied wavelength with the surface/subsurface observed. Moreover, the linear feature in Cosmo-SkyMed image is clearer than PALSAR owing to the high spatial resolution of the former (3 m) versus the latter (16 m).

Then, thematic archaeological layer up to 2000 (highlighted by black spots) and TanDEM-X DEM were synergistically used for the site archaeological investigations, for example, the recognition for the suspected linear feature ([Figure 7](#)). It is evident that the archaeological settlements are distributed on the east along the linear feature (highlighted by pink lines). Other studies ([Xinhuanet 2015](#)) have noted that the Niya ruins site was a swampy alluvial area during Western-Han Dynasty. Consequently, settlements were preferentially located at the terraced platform of the river with a higher elevation to avoid floods. It implied that the ancient Niya River ran through the ruin on the west side, and the linear feature could be interrelated as a section of flood fortifications. In order to further verify this assumption, eight horizontal profiles were drafted on the TanDEM-X DEM data to calculate the height difference between the west and east along suspected fortifications.

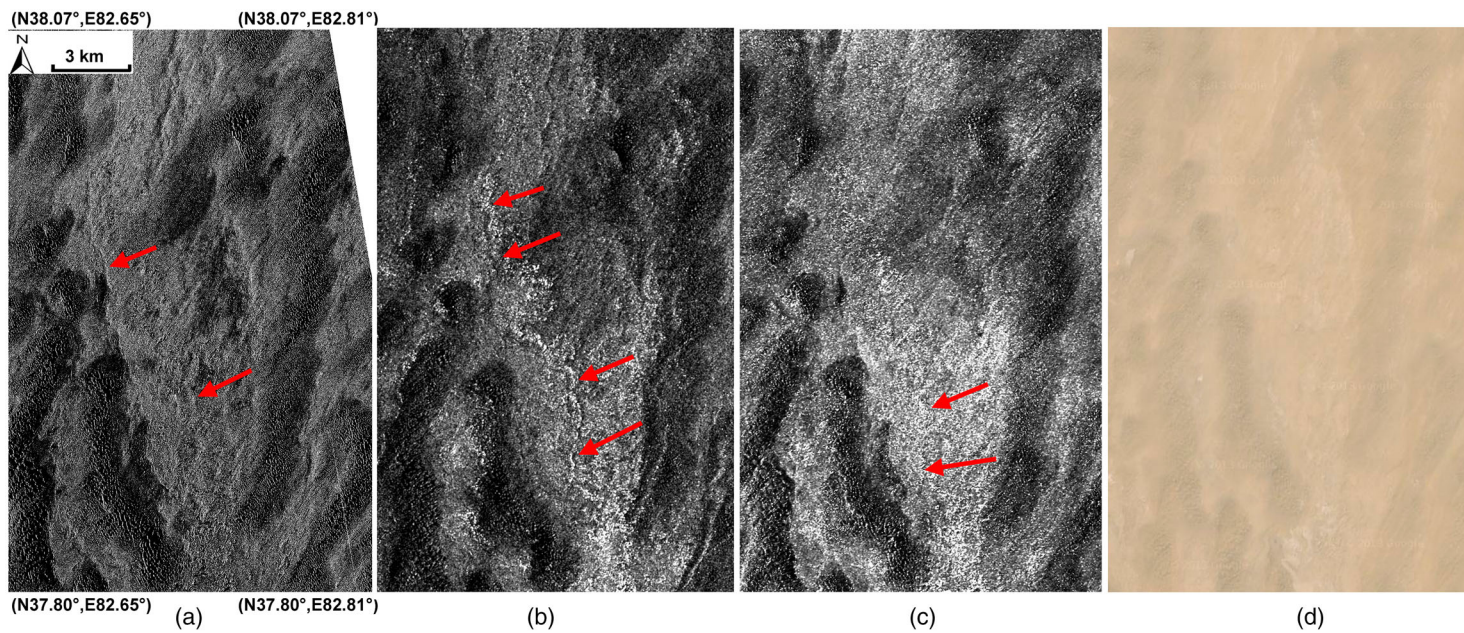


Figure 6. X-, C- and L-band SAR data for the discovery of suspected linear features. (a) X-band Cosmo-SkyMed, (b) C-band Sentinel-1, (c) L-band PALSAR and (d) optical imagery from Google Earth. The discernable archaeological linear features in SAR images were marked by red arrows.

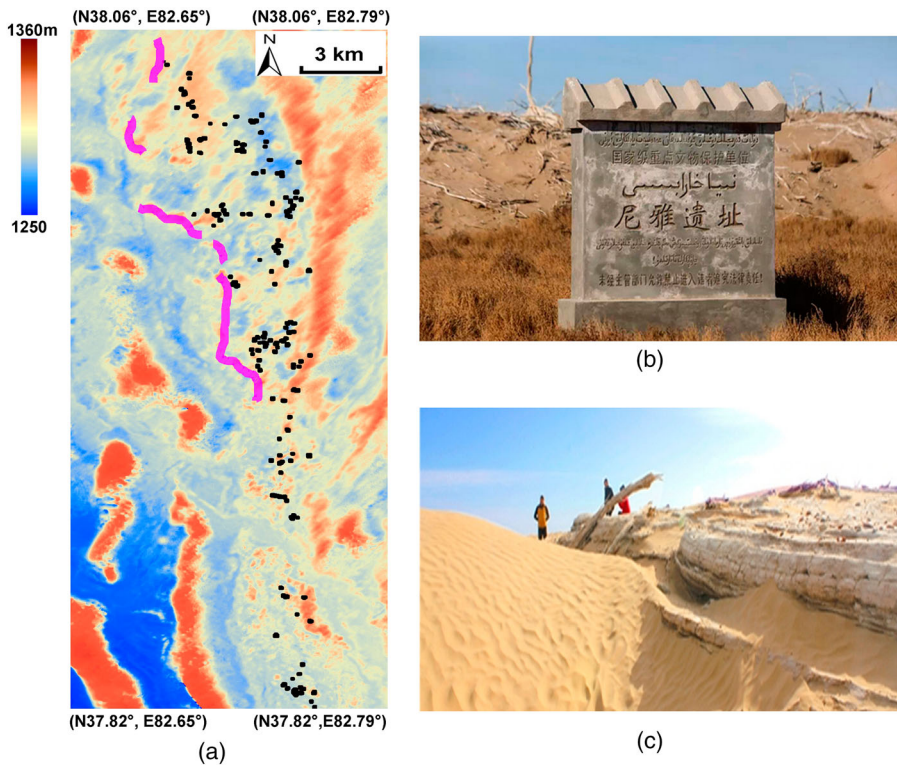


Figure 7. (a) Interpretation of ancient flood fortifications (highlighted by pink lines) uses thematic archaeological layer (black patches) and TanDEM-X DEM data; (b) entrance of Niya site and (c) on-site evidence of the flood fortification along ancient Niya River.

Statistical analysis confirms the lower elevation (i.e. 3.18 m) on the west compared with the east (see Table 2). Some evidences related to flood fortification relics could also be found in field investigations, as shown in (c).

6. Discussion

The reconnaissance of typical archaeological marks (such as crop, shadow and soil/damp marks) by using radar is more complex respect to optical imaging due to a greater number of parameters that characterize SAR data, including (i) characteristics of the radar system as, operating frequency, angles, viewing geometry (ascending or descending), etc. (ii) characteristics of the surface, in

Table 2. Elevation comparison between the west and east of eight profiles across the flood fortifications discovered along the ancient Niya River.

West height (m)	East height (m)	Difference (m)
1259.0	1263.9	4.9
1258.6	1264.2	5.6
1258.2	1262.2	4.0
1259.1	1262.5	3.4
1259.2	1260.8	1.6
1259.5	1260.7	1.2
1258.2	1261.3	3.1
1254.8	1256.4	1.6
Average difference = 3.18 m		

terms of land cover type, topography, relief, dielectric constant, moisture content, conductivity; (iii) archaeological features in terms of buried or emerging remains, their geometric structure, orientation, etc.

Many of these characteristics or parameters are closely interrelated so that the brightness of features and in turn the visibility of archaeological marks is usually linked to several variables. The parameters that have a key role in the interactions between radar and target are: (i) surface roughness, (ii) radar viewing and surface geometry relationship, (iii) moisture content and dielectrical properties of the target. The roughness is usually the dominant factor in a radar picture, but it is very important to consider that it is not an absolute characteristic but it depends on the wavelength and on the incidence angle of radar signal which is another crucial parameter. As a general rule, for the same target in the same conditions, there are significant variations of backscattering by changing the incidence angle of the illuminating wave. Another important parameter is moisture content which strongly affects the electrical properties of soil and therefore, it influences the absorption, transmission and reflection of microwave energy. Generally, radar image brightness tends to increase with an increase in moisture content. A promising approach is based on the multi-temporal amplitude data processing particularly when SAR image acquisition covers an entire plant growth cycle (Stewart, Lasaponara, and Schiavon 2014). However, single data analyses (Linck et al. 2013; Chen, Lasaponara, et al. 2015; Chen, Masini, et al. 2015) can provide excellent results with the use of adequate filtering methods to reduce the impact of noise enhancing subtle features. Generally, the discriminability of archaeological marks is a complex issue linked both to the ratio signal–noise and to the differential scattering behaviour between target/feature and its surrounding. Some recent applications (Chen, Lasaponara, and Masini 2015; Chen, Lasaponara, et al. 2015; Chen, Masini, et al. 2015) suggest a strategy based on the use of (i) adequate filtering techniques, (ii) multi-temporal data processing (Morrison 2013), (iii) knowledge of the problem/site to select the best data and period of observation. Actually, one critical aspect, particularly pressing in archaeology and palaeo-environmental studies, is still today linked with the data-processing issues and approaches which should be adjusted and adapted for archaeological purposes as well as the lack of studies and investigations based on the jointly use of diverse satellite radar sensors providing data in X-, C-, L-band.

In this study, multi-mode products of X-band TerraSAR and Cosmo-SkyMed, C-band Sentinel-1 and L-band PALSAR were analysed in order to evaluate their capability in the identification and monitoring of archaeological remains, particularly taking advantage of the strong backscattering from regular-emerging features and the penetration capability in detection relics shallowly buried. For this purpose, two important archaeological sites were investigated: (i) the Yumen Frontier Pass, successfully added to the World Heritage List On June 22 2014; and (ii) the Niya ruin of Jingue regime, that became a state protected cultural relic site in 1996. Considering the year-round arid-dry environment, the temporal variation of remaining properties (e.g. moisture) is generally ignorable.

For the first test site (the Yumen Frontier Pass with emerging remains), the analysis based on single radar scene pointed out that the linear Great Wall was better detected from SAR data (enhanced echoes from the linear feature dominated by the dihedral backscattering) compared to optical remotely sensed imagery (suppressed spectrum discrimination between the archaeological feature and its surroundings because of the analogous physical properties of materials), as illustrated in Figure 3. Furthermore, the Great Wall was better discernable from X-band TerraSAR (3 and 1 m) and from L-band PALSAR (8 m) scenes, whereas, as evident from a visual comparison of Figure 4, sentinel-1 (20 m) completely missed the Great Wall, the roads and the others man-made structures due to its lower spatial resolution. X-band TerraSAR in the Stripmap mode performs better in its ascending orbit (being the wall in the North–South direction and therefore parallel to the satellite movement), whereas the use of X-band TerraSAR in the Spotlight mode was able to capture the Great Wall also in its descending orbit thanks to its higher spatial resolution and smaller acquisition angle (that also emphasizes the presence of the wall) compared to that of the Stripmap acquisitions.

The multi-date products confirm the ability of PALSAR in the identification of the Great Wall as evident from the average product and from the RGB colour composites (Figure 5c and 5d). They provide, respectively, the clear identification of both archaeological remains and other recent man-made features as well as the changes occurred from one date to another (Figure 5d). Finally, both the interferometric coherence and the image ratios did not provide any easily identifiable information (Figure 5a and 5b).

For the second test site (Niya ruins with subsurface remains), the analysis based on single radar scene pointed out that that all the three sensors X-band Cosmo-SkyMed, C-band Sentinel-1 and L-band PALSAR were able to capture subsurface features compared to optical remotely sensed imagery, such as the linear flood fortifications (Figure 6) along ancient Niya River newly detected by the multi-frequency SAR data. There are many conditions that permit subsurface imaging, among them the most important are (i) the smoothness (barren, plain area) according to the radar band, (ii) the presence of fine grained and homogeneous cover, (iii) the extreme dry desert conditions (less than about 1% moisture) such that even X-band Cosmo-SkyMed was able to penetrate, and finally (iv) the subsurface that should be rough or characterized by higher dielectric contrast. The visibility of flood fortifications buried and/or partially buried by desert sand (see Figure 7c) was of course linked to specific characteristics of each sensor, including the spatial resolution, the acquisition bands, the SNR of imaging as well as the angles. One of the most important parameters is the different penetration capability expected from the diverse sensors being that greater the wavelength greater the penetration depth (Ulaby, Moore, and Fung 1982). So the greater visibility is due to the greater penetration of the L-band compared to the X-band and of course, compared to the Sentinel 1 scene, also to the higher SNR of imaging. Note that, the spatial resolution is no longer the priority in detection large-scale linear features; instead, the discriminability of physical backscattering between archaeological remains and the surroundings become more significant.

7. Conclusion

Since the first entry along the Silk Road comprising sites of China, Kazakhstan and Kyrgyzstan into the World Heritage List in 2014 (i.e. 5000 km stretch of the Silk Road network from Central China to the Central Asia), archaeological prospection along the routes network is increasingly attracting archaeologists, scientists and government officials, particularly in the context of the implementation of the SREB initiative of the Chinese Government. Owing to the characteristics of large scale, penetration and interferometry, SAR remote sensing could be a promising archaeological tool on this vast cultural Corridor characterized by an arid-sandy environment. In this study, archaeological investigations in the Western Regions in Western-Han Dynasty along the Silk Road, in particularly focusing on the Yumen Frontier Pass and the Niya ruin site, were conducted using X-band TerraSAR and Cosmo-SkyMed, C-band Sentinel-1 and L-band ALOS PALSAR data by applying the packaged single-date and multi-temporal SAR data-processing methods. The capability of prevalent spaceborne SAR data for archaeological prospection has been firstly assessed from aspects of spatial resolution, imaging geometry, bands, change detection and monitoring. Results reported in this study highlight the potential and the need to make SAR operative for archaeological research, particular in vast regions with arid-desert environments. More studies and investigations on a variety of archaeological sites with ground truth validations along the Silk Road connecting China to Europe could be a desirable goal for future collaboration among archaeologists, as the implementation of SREB gathers momentum over the coming years and decades. Moreover, establishing a space-to-ground methodology framework of radar remote sensing in archaeology would be the focus of future works that is applicable in variant environmental landscapes and extended chronological stages (e.g. Neolithic and Bronze Age), taking advantage of the technology development of radar sensors as well as data-processing algorithms.

Acknowledgements

The authors wish to acknowledge the anonymous reviewers for providing helpful suggestions that greatly improved the manuscript.

Funding

This work was supported by funding from Hundred Talents Program of the Chinese Academy of Sciences (CAS) [Y5YR0300QM], Youth Director Fund Category-A of Institute of Remote Sensing and Digital Earth, CAS, and the Italian Ministry of Foreign Affairs in the framework of the Great Relevance Project ‘Smart management of cultural heritage sites in Italy and China: Earth Observation and pilot projects’. PALSAR data in Xinjiang Uygur Autonomous Region, China were provided by the European Space Agency (ESA) through the Category-1 Project Id. 28640. TerraSAR-X data were provided by Deutschen Zentrums für Luft- und Raumfahrt (DLR) through the TanDEM-X Science proposal CAL_VAL6905. The archaeological layer of Niya ruin was from Archaeological Institute of Xinjiang Uygur Autonomous Region, China.

Disclosure statement

No potential conflict of interest was reported by the authors.

References

- Agapiou, A., and V. Lysandrou. 2015. “Remote Sensing Archaeology: Tracking and Mapping Evolution in European Scientific Literature from 1999 to 2015.” *Journal of Archaeological Science: Reports* 4: 192–200.
- Ashmore, W., and C. Blackmore. 2008. “Landscape Archaeology.” In *Encyclopedia of Archaeology*, edited by D. M. Pearsall, 1569–1578. New York: Academic Press.
- Boldt, M., and K. Schulz. 2012. “Change Detection in High Resolution SAR Images: Amplitude Based Activity Map Compared with the CoVAmCoh Analysis.” In *Proceedings of the Geoscience and Remote Sensing Symposium (IGARSS)*, 3803–3806. Munich, Germany: IEEE.
- Bonavia, J. 2004. *The Silk Road from Xi'an to Kashgar*. Revised by Christoph Baumer. Hong Kong: Odyssey Publications.
- Chen, F., R. Lasaponara, and N. Masini. 2015a. “An Overview of Satellite Synthetic Aperture Radar Remote Sensing in Archaeology: From Site Detection to Monitoring.” *Journal of Cultural Heritage*, in press (Available online 22 June 2015). doi:10.1016/j.culher.2015.05.003.
- Chen, F., R. Lasaponara, N. Masini, and R. Yang. 2015b. “Satellite SAR Data Assessment for Silk Road Archaeological Prospection.” *EGU General Assembly, Geophysical Research Abstracts* 17: EGU2015–10059.
- Chen, F., N. Masini, R. Yang, P. Milillo, D. Feng, and R. Lasaponara. 2015c. “A Space View of Radar Archaeological Marks: First Applications of COSMO-SkyMed X-Band Data.” *Remote Sensing* 7: 24–50.
- Cigna, F., D. Tapete, R. Lasaponara, and N. Masini. 2013. “Amplitude Change Detection with Envisat ASAR to Image the Cultural Landscape of the Nasca Region, Peru.” *Archaeological Prospection* 20: 117–131.
- Crawford, O.G.S. 1929. “Air Photography for Archaeologists.” *Ordnance Survey Professional Papers*, new series, 12, HMSO, Southampton.
- Erasmi, S., R. Rosenbauer, R. Buchbach, T. Busche, and S. Rutishauser. 2014. “Evaluating the Quality and Accuracy of TanDEM-X Digital Elevation Models at Archaeological Sites in the Cilician Plain, Turkey.” *Remote sensing* 6: 9475–9493.
- Garrison, T. G., B. Chapman, S. Houston, E. Roman, and J. L. G. Lopez. 2011. “Discovering Ancient Maya Settlements Using Airborne Radar Elevation Data.” *Journal of Archaeological Science* 38: 1655–1662.
- Goldstein, R. M., and C. L. Werner. 1998. “Radar Interferogram Filtering for Geophysical Applications.” *Geophysical Research Letters* 25: 4035–4038.
- Hill, J. E., and Y. Fan. 2009. *Through the Jade Gate to Rome: A Study of the Silk Routes During the Later Han Dynasty, 1st to 2nd Centuries CE*. Charleston, SC: BookSurge.
- Keay, S. J., S. H. Parcak, and K. D. Strutt. 2014. “High Resolution Space and Ground-Based Remote Sensing and Implications for Landscape Archaeology: The Case From Portus, Italy.” *Journal of Archaeological Science* 52: 277–292.
- Lasaponara, R., and N. Masini. 2013. “Satellite Synthetic Aperture Radar in Archaeology and Cultural Landscape: An Overview.” *Archaeological Prospection* 20: 71–78.
- Lasaponara, R., and N. Masini. 2015. “Reconnaissance of Archaeology Marks Through Satellite Synthetic Aperture Radar.” In *Detecting and Understanding Historic Landscapes*, edited by A. Chavarria and A. Reynolds, 93–108. Mantiva, Italy: SAP Società Archeologica s.r.l.

- Lee, J.-S. 1980. "Digital Image Enhancement and Noise Filtering by Use of Local Statistics." *IEEE Transactions on Pattern Analysis and Machine Intelligence* 2: 165–168.
- Linck, R., T. Busche, S. Buckreuss, J. Fassbinder, and S. Seren. 2013. "Possibilities of Archaeological Prospection by High-Resolution X-Band Satellite Radar – A Case Study from Syria." *Archaeological Prospection* 20: 97–108.
- Liu, J., D. Guo, Y. Zhou, Z. Wu, W. Li, F. Zhao, and X. Zheng. 2011. "Identification of Ancient Textiles from Yingpan, Xinjiang, by Multiple Analytical Techniques." *Journal of Archaeological Science* 38: 1763–1770.
- Liu, S., Q. H. Li, F. Gan, P. Zhang, and J. W. Lankton. 2012. "Silk Road Glass in Xinjiang, China: Chemical Compositional Analysis and Interpretation Using a High-Resolution Portable XRF Spectrometer." *Journal of Archaeological Science* 39: 2128–2142.
- Lopes, A., R. Touzi, and E. Nezry. 1990. "Adaptive Speckle Filters and Scene Heterogeneity." *IEEE Transactions on Geoscience and Remote Sensing* 28: 992–1000.
- Luo, L., X. Wang, C. Liu, H. Guo, and X. Du. 2014. "Integrated RS, GIS and GPS Approaches to Archaeological Prospecting in the Hexi Corridor, NW China: A Case Study of the Royal Road to Ancient Dunhuang." *Journal of Archaeological Science* 50: 178–190.
- Masini, N., and R. Lasaponara. 2007. "Investigating the Spectral Capability of QuickBird Data to Detect Archaeological Remains Buried Under Vegetated and not Vegetated Areas." *Journal of Cultural Heritage* 8: 53–60.
- McCauley, J. F., G. G. Schaber, C. S. Breed, M. J. Grolier, C. V. Haynes, B. Issawi, C. Elachi, and R. Blom. 1982. "Subsurface Valleys and Geoarchaeology of the Eastern Sahara Revealed by Shuttle Radar." *Science* 218: 1004–1020.
- Morrison, K. 2013. "Mapping Subsurface Archaeology with SAR." *Archaeological Prospection* 20: 149–160.
- Narayanan, R. M., and P. P. Hirsave. 2001. "Soil Moisture Estimation Models using SIR-C SAR Data: A Case Study in New Hampshire, USA." *Remote Sensing of Environment* 75: 385–396.
- Nico, G., M. Pappalepore, G. Pasquariello, A. Refice, and S. Samarelli. 2000. "Comparison of SAR Amplitude vs. Coherence Flood Detection Methods—a GIS Application." *International Journal of Remote Sensing* 21: 1619–1631.
- Parcak, S. H. 2009. *Satellite Remote Sensing for Archaeology*. Abingdon & New York: Routledge.
- Ranson, K. J., G. Sun, V. I. Kharuk, and K. Kovacs. 2001. "Characterization of Forests in Western Sayani Mountains, Siberia from SIR-C SAR Data." *Remote Sensing of Environment* 75: 188–200.
- Rondelli, B., S. Stride, and J. J. Garcia-Granero. 2013. "Soviet Military Maps and Archaeological Survey in the Samarkand Region." *Journal of Cultural Heritage* 14: 270–276.
- Schaber, G. C., J. F. McCauley, and C. S. Breed. 1997. "The Use of Multifrequency and Polarimetric SIR-C/X-SAR Data in Geologic Studies at BirSafsaf, Egypt." *Remote Sensing of Environment* 59: 337–363.
- Scheuchl, B., T. Ullmann, and F. Koudogbo. 2009. "Change Detection using High Resolution TerraSAR-X Data Preliminary Results." *The International Archives of the Photogrammetry, Remote Sensing and Spatial Information Sciences XXXVIII-1-4-7/W5*, Hannover, Germany, June 2–5.
- Shi, J., Y. Du, J. Du, L. Jiang, L. Chai, K. Mao, P. Xu, W. Ni, C. Xiong, Q. Liu, et al. 2012. "Progress on Microwave Remote Sensing of Land Surface Parameters." *Science China Earth Sciences* 55: 1052–1078.
- Shi, Z., and K. B. Fung. 1994. "A Comparison of Digital Speckle Filters." In *Proceedings of the IGARSS 94*, 2129–2133. Pasadena, CA: IEEE.
- Stewart, C., R. Lasaponara, and G. Schiavon. 2013. "ALOS PALSAR Analysis of the Archaeological Site of Pelusium." *Archaeological Prospection* 20: 109–116.
- Stewart, C., R. Lasaponara, and G. Schiavon. 2014. "Multi-frequency, Polarimetric SAR Analysis for Archaeological Prospection." *International Journal of Applied Earth Observation and Geoinformation* 28: 211–219.
- Ulaby, F. T., R. K. Moore, and A. K. Fung. 1982. *Microwave Remote Sensing*. Vol. II. Reading, MA: Addison-Wesley.
- Wang, S., and X. Zhao. 2013. "Re-evaluating the Silk Road's Qinghai Route using Dendrochronology." *Dendrochronologia* 31: 34–40.
- Xinhuanet. 2015. "The ten major enigmas in Xinjiang." Accessed April 20, 2015, from <http://www.xj.xinhuanet.com/sdzm/nyzm/nyzm.htm>
- Yilmaz, H. M., M. Yakar, and F. Yildiz. 2008. "Documentation of Historical Caravansaries by Digital Close Range Photogrammetry." *Automation in Construction* 17: 489–498.